ARTICLE

OBC
www.rsc.org/obc

The type I rat fatty acid synthase ACP shows structural homology and analogous biochemical properties to type II ACPs

Michelle A. C. Reed,[a] Michael Schweizer,†[c] Anna E. Szafranska,[a] Chris Arthur,[a] Thomas P. Nicholson,[a] Russell J. Cox,[a] John Crosby,*[a] Matthew P. Crump*[b] and Thomas J. Simpson[a]

[a] *School of Chemistry, University of Bristol, Cantock's Close, Bristol, UK BS8 1 TS. E-mail: john.crosby@bris.ac.uk*

[b] *Division of Biochemistry and Molecular Biology, School of Biological Sciences, University of Southampton, Bassett Crescent East, Southampton, UK S016 7PX. E-mail: m.p.crump@soton.ac.uk*

[c] *Genetics and Microbiology Department, Institute of Food Research, Norwich Research Park, Colney, Norwich, UK NR4 7UA*

Received 16th September 2002, Accepted 27th November 2002
First published as an Advance Article on the web 3rd January 2003

While X-ray and NMR structures are now available for most components of the Type II fatty acid synthase (FAS), there are no structures for Type I FAS domains. A region from the mammalian (rat) FAS, including the putative acyl carrier protein (ACP), has been cloned and over-expressed. Here we report multinuclear, multidimensional NMR studies which show that this isolated ACP domain contains four α-helices (residues 8–16 [1]; 41–51 [2]; 58–63 [3] and 66–74 [4]) and an overall global fold characteristic of ACPs from both Type II FAS and polyketide synthases (PKSs). ‡ The overall length of the structured ACP domain (67 residues) is smaller than the structured regions of the *Eschericia coli* FAS ACP (75 residues), the actinorhodin PKS ACP (78 residues) and the *Bacillus subtilis* FAS ACP (76 residues). We further show that the rat FAS ACP is recognised as an efficient substrate by enzymes known to modify Type II ACPs including phosphopantetheinyl and malonyl transferases, but not by the heterologous *S. coelicolor* minimal polyketide synthase.

1. Introduction

Acyl carrier proteins are small proteins, which play a key role in fatty acid biosynthesis. These proteins have been found in a diverse range of organisms including bacteria,[1] plants,[2] insects[3] and mammals[4] where their main role is to chaperone the extending fatty acyl chain and, on chain completion, to act as a donor of mature fatty acids to diverse biosynthetic processes.[5] In bacteria and plants each cycle of condensation, dehydration and further reduction is catalysed by a group of monofunctional polypeptides (the Type II FAS),[6] while large multifunctional enzymes (Type I synthases) found in fungi and animals perform similar biosynthetic cycles.[4,7] In both Type I and Type II FASs the functional form of the ACP contains a 4′-phosphopanthetheine prosthetic group derived from CoA, which is attached by the enzyme *holo*-ACP synthase (ACPS) to a conserved serine residue within the carrier protein.[8] The terminal phosphopanthetheinyl sulfhydryl provides the site of covalent attachment for the growing fatty acyl chain.

Similar carrier proteins are associated with other acyl transfer dependent pathways including the synthesis of polyketides,[9] non ribosomally synthesised peptides,[10] lipopeptides,[11] acylation and synthesis of oligosaccharides[12] and the production of D-alanyl lipoteichioc acid.[13] Acyl carrier proteins play a central role in these biosynthetic pathways by recognizing and associating with several different enzymes during the biosynthesis. There is therefore an obvious need for structural information on these proteins.

NMR studies have provided solution structures for Type II ACPs from *E.coli* FAS,[14] spinach FAS,[15] *Bacillus subtilis* FAS,[16] rhizobium NodF carrier protein,[17] *Streptomyces coelicolor* actinorhodin (act) polyketide synthase (PKS),[18] and the Type I modular peptidyl carrier protein from *Bacillus brevis*.[19] These studies have suggested that carrier proteins have a common structure consisting of a four α-helical bundle with the conserved serine phosphopantetheine attachment site located at the base of the second helix. Where the structures have been studied, the *apo* and 4′-phosphopantetheine containing *holo* forms of these Type II proteins look identical. Recent crystal structures have also indicated the site of protein–protein interaction between the *B. subtilis* ACP and ACPS[20] (a site proposed for the interaction of all discrete FAS proteins),[21] and the positioning of the phosphopantetheine bound acyl group within the hydrophobic cavity of *E. coli* ACP.[22] Given the overall similarities of the carrier protein three-dimensional structures it was initially suggested that ACPs from either different organisms[23] or different biosynthetic pathways[24] could be interchanged, either *in vivo* or *in vitro*, to give functioning protein complexes. More recently, however, work on FAS enzymes from a number of organisms,[25–27] as well as the *in vitro* minimal PKS assay[28] have highlighted examples where ACP substitution resulted in an inactive protein complex. In these cases subtle differences in structure must be evident and detailed comparisons of carrier proteins from a range of organisms and biosynthetic pathways are required to illuminate the differences underlying these functional changes.

At present there is no structure available for a Type I FAS ACP. Previously Tropf *et al.*[29] cloned a region from the rat FAS gene corresponding to the putative ACP domain and demonstrated expression in *E. coli* of a soluble protein with a mass of 9686 Da. This agreed with the calculated mass for the *apo*-form of the protein minus the *N*-terminal methionine. The proportion of *holo*-ACP present was estimated to be about 1% of the total ACP obtained. It has been reported by Tropf *et al*. that co-expression of the rat ACP with *E. coli* ACPS produced a

† *Present address*: School of Life Sciences, Heriot-Watt University, Edinburgh, UK EH14 4AS.

‡ The average minimized coordinates for the rat FAS ACP have been deposited in the protein data bank with access code 1N8L.

DOI: 10.1039/b208941f

small increase in the overall levels of the active *holo* form of the protein. *E. coli* ACPS is thought to be relatively intolerant to ACP substrates but it has been effectively used to post-translationally modify FAS and PKS ACPs both *in vivo*[30,31] and *in vitro*.[32] *In vitro* incubation of purified rat FAS ACP with *E. coli* ACPS and CoA, however, completely converted the inactive *apo*-ACP to the active *holo* form.[29] The active Type I rat FAS ACP was modified by several Type II FAS enzymes including malonyl CoA:ACP transacylase (MCAT) and it was reported that this Type I FAS ACP could functionally replace *in vivo* the actinorhodin PKS ACP, though product production here was estimated at only 1% of control experiments. These results suggested that the rat FAS ACP was folded into a conformation similar to that seen for Type II ACPs.

In the present study we have structurally characterised recombinant rat ACP by CD and multinuclear, multi-dimensional NMR studies to show that this isolated domain adopts a pH stable folded structure. The rat FAS ACP appears to have a similar global fold to published ACP structures. This provides the first evidence for significant structural similarity between a Type I FAS domain and a Type II acyl carrier protein. The ACP domain of the Type I rat FAS is modified by the *E. coli* ACPS *in vivo*, and the *S. coelicolor* ACPS *in vitro* as well as the *S. coelicolor* MCAT all of whose natural targets are Type II enzymes. However, in an *in vitro* minimal Type II PKS assay,[28] rat FAS ACP could not functionally replace *act* PKS ACP in the production of the polyketides SEK 4 and SEK 4b.

2. Materials and methods

2.1 Bacterial strains, plasmids and media

An open reading frame (ORF) encoding amino acids 2114–2202 of the rat FAS was constructed between the *Nde*I and *Bam*H1 sites of pET15b (Novagen).[29] The 409 bp BgIII fragment from pRJC005 containing the ACPS gene from *E. coli*[30] was ligated with pET15b-ACP which had been enzymically cut using *Bam*Hl. The resulting ligation was transformed into *E. coli* DH5α and single colonies were checked for a correctly oriented insert by digestion of plasmid DNA with *Xba*I and *Sac*I. *E. coli* strains DH5α and BL21(DE3) were used for plasmid manipulation and expression of cloned genes respectively.

2.2 Expression of the ACP domain of rat FAS

E. coli cells were grown in Luria-Bertani (LB) media containing 100 μg ml^{-1} carbenicillin at 37 °C (orbital shaker speed 250 rpm). A single colony from freshly transformed BL21(DE3) was grown overnight in 100 ml LB and aliquots (2.5 ml) from this flask were used to inoculate growth flasks. The cells were grown until an absorbance ($A_{595\ nm}$) of 0.6 was obtained and then induced by adding isopropyl β-D-thiogalactopyranoside (IPTG) to a final concentration of 1 mM. After four hours, the cells were recovered by centrifugation (4500 g, 10 min, 4 °C). The cell pellet was then resuspended in Tris-Cl buffer (50 mM, pH 8.0 containing 10% glycerol) and frozen.

2.3 Expression of a ^{15}N-labelled *apo*-ACP domain of rat FAS

20 Flasks containing 100 ml LB media (100 μg ml^{-1} carbenicillin) were inoculated and the cells grown until an absorbance ($A_{595\ nm}$) of 1.2 was reached. The bacteria were pelleted by centrifugation (5500 g, 4 °C, 15 min) and washed with 100 ml M9 minimal media before further centrifugation (5500 g, 4 °C, 15 min). The pellet was resuspended in 50 ml of M9 minimal media and 2.5 ml of this suspension was used to inoculate twenty 500 ml flasks each containing 100 ml of M9 media containing $^{15}NH_4C1$ (1 g L^{-1}) and carbenicillin (100 μg ml^{-1}). Expression was induced using IPTG as described previously. Bacteria were grown for a further 18 hours at 37 °C (250 rpm) before being harvested as described above.

2.4 Purification of the ACP domain of rat FAS

Cytosolic proteins were extracted from the cells using a freeze–thaw method.[33] Typically, cells from 4 L LB media were frozen at −78 °C and then slowly thawed with the addition of 100 ml 50 mM Tris-Cl buffer (pH 8.0). Bacterial cells were removed by centrifugation (5500 g, 4 °C, 15 min), and protein precipitated from the resulting supernatant by a 0–60% ammonium sulfate cut was discarded following centrifugation (6800 g, 10 min, 4 °C). The ammonium sulfate concentration was then increased to 90%, the pH adjusted to pH 4.0 with 2 M HCl and the suspension was left at 4 °C to allow the protein to flocculate. Following centrifugation (25000 g, 20 min, 4 °C), the pellet was resuspended in a minimal volume of 50 mM Tris-Cl buffer and the pH adjusted to pH 8.0. This solution was desalted on an HR 16/10 fast desalt column (Pharmacia) and applied to a HiLoad™ 26/10 Q Sepharose® column (Pharmacia). Both columns were equilibrated in 50 mM Tris buffer (pH 8.0). Bound protein was eluted (2 ml min^{-1}) over a 400 ml gradient of 0–1 M NaCl. Fractions shown by 17.5% SDS–PAGE to contain only rat ACP were freeze-dried and then desalted into Milli-Q water using an HR10/10 fast desalt column (Pharmacia). Purified protein samples were prepared for mass spectrometric analysis using the method of Winston and Fitzgerald.[34] All analyses were done using a Micromass Quattro mass spectrometer equipped with an electrospray source as described previously.[35]

2.5 Circular dichroism

All CD experiments were done at 20 °C on 5 μM (0.05 mg ml^{-1}) protein solutions in a 1 ml CD Quartz cell (Helma, 2 mm path length) using a Jobin Yvon CD 6 spectropolarimeter. Molecular ellipticity was recorded over the range pH 1 to pH 7 and also with 0–6 M guanidinium hydrochloride at pH 5.5 for wavelengths 190–260 nm.

2.6 *Holo*-acyl carrier protein synthase assay

S. coelicolor ACPS was expressed in *E. coli* and purified as a His tagged protein.[23] A typical phosphopantetheinylation assay contained 50 μM *apo*-ACP, 1 μM *S. coelicolor* His_6-ACPS, 0.5 mM CoA, 10 mM $MgCl_2$, 5 mM DTT and 50 mM Tris-Cl buffer (pH 8.8). The assay components were mixed and incubated at room temperature overnight, after which the progress of the reaction was determined by ESMS. The resultant *holo*-ACP sample was then desalted into water (Fast Desalt HR 10/10 column) and re-purified by anion exchange chromatography. Acetyl rat FAS ACP, was prepared by replacing CoA with acetyl CoA. Protein samples were desalted and analysed by ESMS as described above.

2.7 Malonylation of the rat FAS ACP catalysed by *S. coelicolor* malonyl CoA:ACP transacylase

S. coelicolor His_6-MCAT was purified as described previously.[36] Transfer of the malonyl residue from malonyl CoA to *holo*-ACPs formed the basis of the assay method. Typically, assay solutions contained 50 μM *holo*-ACP, 50 μM malonyl CoA, 0.1 mM DTT, 50 mM phosphate buffer (pH 6.5) and 1 nM His_6-MCAT (46.5U mg^{-1} where one unit of His_6-MCAT is defined as the amount of protein required to catalyze the synthesis of 1 pmol of malonyl ACP per second at pH 6.5 and 30 °C) in 100 μL. Prior to use, ACP was reduced with DTT (1 mM) (2 hours, 30 °C) and pre-incubated with the MCAT for 15 minutes. Addition of malonyl CoA to the assay was followed by incubation under the same conditions for 2 hours. The extent of malonylation was determined following analysis by ESMS. Malonyl SNAC was synthesized using methods described previously.[37] Concentrations of up to 1 mM malonyl SNAC replaced malonyl CoA in the normal assay.

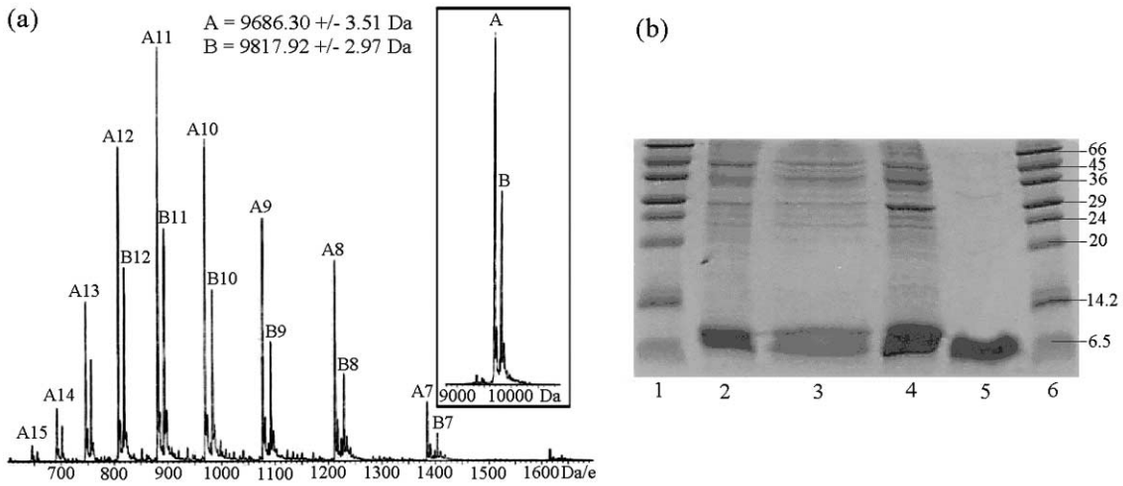

Fig. 1 **(a)** ESMS of the rat ACP domain: peak A, mass 9686.3 Da (expected mass of rat *apo*-ACP (−Met) = 9686 Da); peak B, mass 9817.9 Da (expected mass of rat *apo*-ACP (+Met) = 9817 Da). The inset to panel A shows the transformed data. **(b)** SDS–PAGE gel (17.5%): lane 1,6: molecular weight markers (kDa); lane 2: freeze–thaw supernatant; lane 3: after 0–60% ammonium sulphate cut; lane 4: the 60–90% ammonium sulphate cut; lane 5: rat *apo*-ACP eluting from Q. sepharose column (0.25 M NaCl).

2.8 Minimal act PKS assay

Typically the assay[28] contained: *holo*-ACP (50 μM), KS/CLF (1 μM), DTT (1.0 mM), EDTA (2 mM), malonyl CoA (1 mM) and 0.1 mM potassium phosphate–10% glycerol, pH 7.3 in a final volume of 100 μL. The assay was performed using rat FAS *holo*-ACP in the presence and absence of *S. coelicolor* MCAT (1 nM). C17S *act holo*-ACP[26] was used as a control. Stock solutions of ACP (500 μM were reduced with DTT (1 mM) at 30 °C overnight. Prior to addition of malonyl CoA, the ACP was incubated with KS/CLF for 10 minutes followed by incubation with malonyl CoA for 2 hours at 30 °C. The reaction was quenched by addition of 50% (w/v) TCA (100 μL) and 100 mg NaH_2PO_4. Polyketide metabolites were extracted with ethyl acetate (3 × 300 μL). The organic extract was pooled, freeze-dried and the residue was re-suspended in 100 μL methanol. HPLC analysis was done using Luna (2) C18 RP-column 250 × 4.6 mm (Phenomenex) eluted at a rate of 1 ml min^{-1} with increasing concentrations of acetonitrile containing 0.05% TFA (v/v). The column was equilibrated for 5 minutes after injection of the sample with water–0.05% TFA (v/v). The concentration of acetonitrile was then linearly increased to 75% over 30 minutes. Eluted peaks were detected by monitoring $A_{280\ nm}$ using a sensitivity of 0.02 absorbance unit full scale (AUFS). SEK4 was eluted at around 20 minutes followed by SEK 4b at around 21 minutes.

2.9 NMR methods

The protein was dissolved to a final concentration of 1–2 mM in D_2O (99.96%) or 10% D_2O–90% H_2O containing 20 mM sodium deuteroacetate, 1 mM NaN_3 and 1 mM DTT, pH or pD 5.5. NMR experiments were performed on a Varian *INOVA* or Unity 600 MHz spectrometer at 25 °C or 35 °C either in the Division of Biochemistry, University of Southampton or at PENCE, University of Alberta. Standard 2D and 3D techniques were employed for the assignment of ^1H and ^{15}N resonances. Spectra acquired included: 3D NOESY–HSQC (150 ms mixing time); TOCSY–HSQC (55 ms mixing time) and HNHA data sets; nuclear Overhauser spectroscopy (NOESY) with mixing times of 50, 100, 140 and 200 ms; total correlation spectroscopy (TOCSY) with a mixing time of 50 ms; and double-quantum filtered correlated spectroscopy (DQF-COSY).

The 3-dimensional structure of the protein was modeled using XPLOR 3.81[38] with a dynamic simulated annealing protocol.[39] The initial structure was subjected to 500 cycles of Powell energy minimization to provide an energetically feasible structure. High temperature dynamics were run for 40 picoseconds at an initial temperature of 1000 K, with each of the calculations initiated using randomized dynamics trajectories. Each structure was analysed for NOE and dihedral angle violations and visualized using Insight II (Accelrys Software). A total of 30 structures were calculated from which 24 structures with converged global folds were selected. A minimized average structure was calculated from the mean coordinates of this set of 24 structures. The local angle geometry was analysed by PROCHECK[40] for the mainchain angles, ϕ and ψ.

3. Results

3.1 Expression and purification of the unlabelled and ^{15}N labeled *apo*-ACP domain of rat FAS

Unlabelled rat *apo*-ACP eluting from the ion exchange column at 0.25 M NaCl was shown to be pure by SDS–PAGE (Fig. 1). The anomalously low molecular weight (6.5 kDa) observed following SDS–PAGE analysis of ACPs has been previously reported.[35] ESMS analysis showed that there was good agreement between the calculated mass for the expressed protein with loss of the *N*-terminal methionine (9686 Da) and the mass observed by ESMS (9686.3 ± 3.5 Da). A small proportion of the rat *apo*-ACP observed by ESMS retained the *N*-terminal methionine and had a molecular mass of 9817.9 ± 2.9 Da which is close to the expected molecular mass of 9817 Da. Approximately 5 mg L^{-1} pure rat FAS ACP were routinely obtained. The same purification procedure was used for the ^{15}N labeled rat FAS ACP. With theoretical 100% incorporation, the molecular mass of ^{15}N-labeled rat *apo*-ACP (−Met) was expected to be 9811 Da, an increase of 125 Da compared with the unlabelled protein. The most intense set of peaks observed by ESMS was 9800.1 ± 0.9 Da, representing 90.4% incorporation of ^{15}N. A low degree of expression before induction led to a small proportion of unlabelled protein also being observed by ESMS. 2 mg L^{-1} of ^{15}N-labelled rat FAS ACP was routinely obtained.

3.2 Circular dichroism studies

The CD spectrum of rat ACP shows an intense negative band at 207 nm and a broad shoulder centred at about 219 nm (Fig 2d). For an infinitely long model α-helix, characteristic negative absorptions at 180, 208 and 222 nm and a positive absorption at 192 nm are observed by CD (Fig. 2a).[41] Since the intensity of CD signals from α-helices is greater than that of β-sheet or random coil in the 200–240 nm range, these signals dominate spectra of proteins with significant α-helical content. Fig. 2d shows that α-helical signal dominates the CD spectrum of the

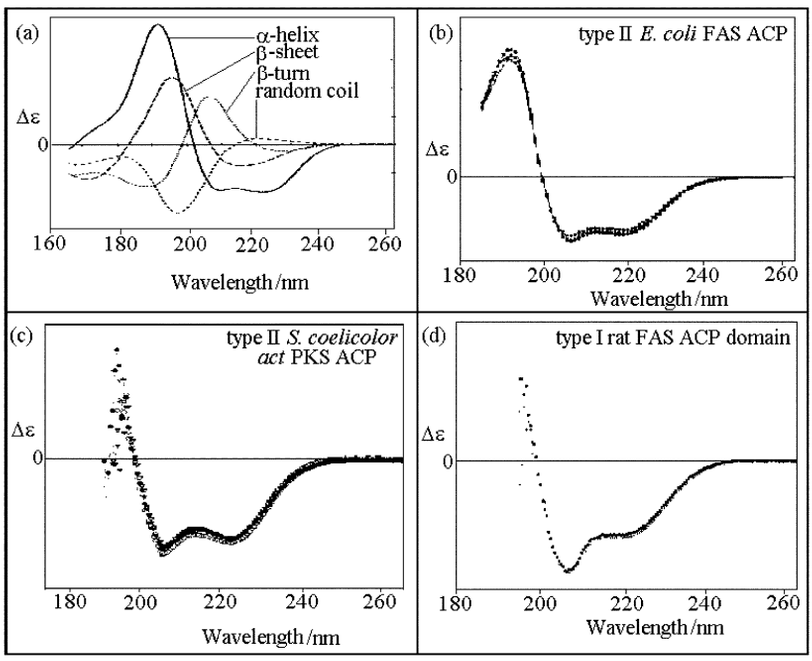

Fig. 2 CD spectra for (a) various secondary structures;[41] (b) Type II *E. coli* FAS ACP at pH 6.1 (varying concentrations of potassium phosphate);[55] (c) Type II *S. coelicolor act* PKS ACP at pH 5.5 (varying concentrations of KCl),[43] (d) the ACP domain of the Type I rat FAS at pH 5.5 and pH 6.0.

rat FAS ACP. The absorption at 219 nm rather than the ideal at 222 nm may result from the helices being short and influenced by other secondary structural elements. The *E. coli* FAS and *S. coelicolor act* PKS Type II ACPs both have a negative absorption near the ideal of 222 nm (Figs 2b and 2c), suggesting greater α-helical content in these proteins.

There is little influence of pH on the structure of the rat FAS protein between the pH range 2–7 (Fig. 3a). Below pH 2, there is evidence of a partial loss of structure. For the Type II PKS ACP from *S. coelicolor*, a loss of native secondary structure below pH 4.5 was observed (Fig. 3b) indicating that the secondary structure of the ACP domain of the Type I rat FAS is more stable to changes in pH.

The far UV CD spectrum changed dramatically between 2 M and 4 M guanidinium hydrochloride (GuHCl) indicating loss of secondary structure. As the GuHCl introduced severe noise into the spectrum below 210 nm the CD signal resulting from the shoulder at 219 nm was used to follow the denaturation of the protein (Fig. 4). This revealed steady loss in α-helical content up to 3 M GuHCl with almost complete denaturing at 6 M GuHCl. The transition is smooth with an apparently uniform loss of secondary structure over the whole of the protein. There is no evidence for the persistence of any single stable element of structure. Similar highly cooperative unfolding in the presence of GuHCl was observed for the Type II ACPs of both the *E. coli* FAS[42] and the *S. coelicolor act* PKS.[43]

3.3 Rat FAS ACP as a substrate for ACPS and MCAT

Co-expression of the rat ACP with *E. coli* ACPS led to the formation of high yields (10 mg L^{-1}) of *holo*-ACP (10026.17 ± 1.26 Da, expected mass (−Met), 10026 Da) suggesting complete post-translational modification of the *apo*-ACP by the heterologous ACPS. *E. coli* ACPS has previously been shown to have a broad substrate specificity.[30,31] This result, however, is contrary to previous reports of poor post translational modification of the rat FAS protein.[29] *In vitro* a catalytic amount of the Type II ACPS from *S. coelicolor* was sufficient to give at least 90% conversion of rat *apo*-ACP to acetyl-ACP in the presence of acetyl-CoA. Phosphopantetheinyl transfer is unaffected by acylation of the phosphopantetheine thiol and ACPS has been used as a tool to produce acyl *holo*-ACPs from *apo*-ACPs

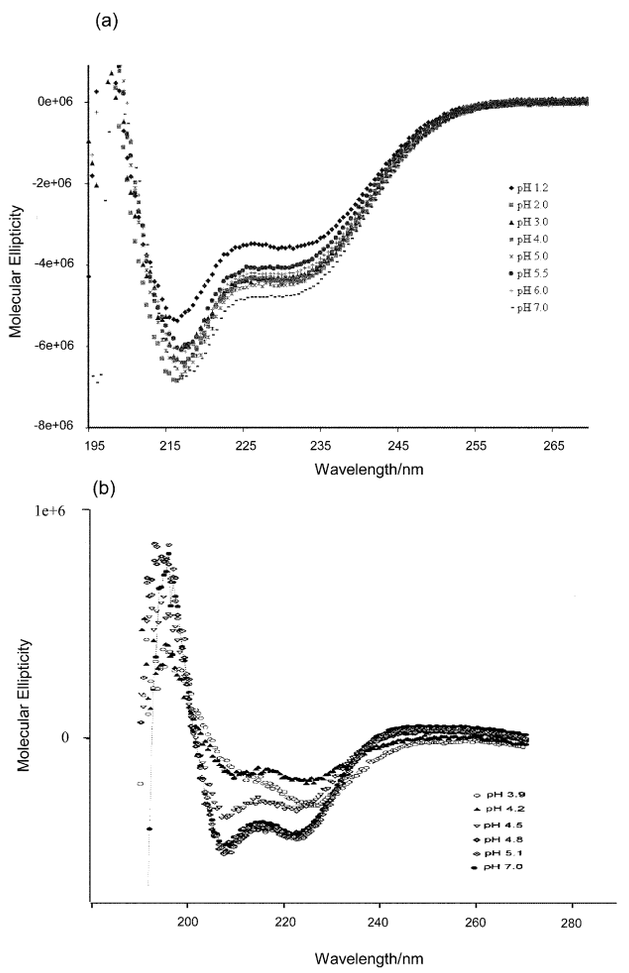

Fig. 3 The far UV CD spectrum of (a) the rat ACP domain over the pH range 1.2–7.0 (b) *act apo*-ACP over the pH range 3.9–7.0.

directly.[30,31] ESMS showed two peaks with masses of 10198.2 ± 2.9 Da and 10066.32 ± 2.38 Da, corresponding to acetyl-ACP with (expected 10198 Da) and without (expected 10068 Da) the *N*-terminal methionine.

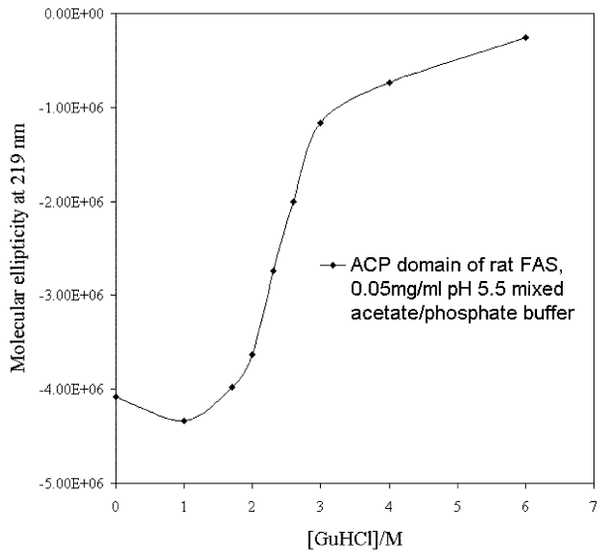

Fig. 4 Effects of increasing denaturant concentration (GuHCl) on rat FAS secondary structure measured at 219 nm.

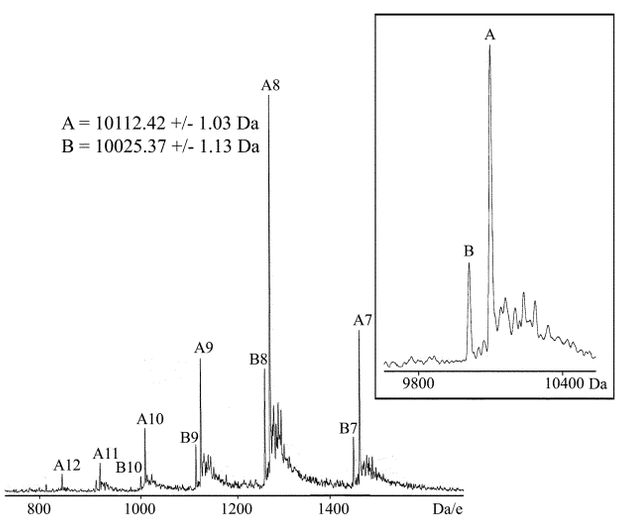

Fig. 5 ESMS showing the transfer of malonyl moieties from malonyl SNAC to rat *holo*-ACP by *S. coelicolor* MCAT (transformed spectrum inset). Peak A mass 10112.4 Da, peak B mass 10025.4 (A, expected malonyl ACP (−Met) 10112 Da; B, expected *holo*-ACP (−Met) 10027 Da).

S. coelicolor His_6-MCAT catalysed the transfer of malonyl moieties from both malonyl-CoA and malonyl SNAC to rat *holo*-ACP to form malonyl-ACP (10112 Da) (Fig. 5). The extent of malonylation, however, depended upon the concentration and source of the malonyl moiety. Approximately a 20-fold greater concentration of malonyl SNAC was required to effect the same extent of malonylation than with the natural co-substrate malonyl CoA under the conditions used.

3.4 Secondary structure and global fold of the Type I rat *apo*-ACP

The ^{1}H and ^{15}N assignments for the rat ACP were derived from the analysis of standard 2D and 3D NMR experiments recorded at 25 °C or 35 °C, pH 5.5. The ^{1}H–^{15}N HSQC spectrum (Fig. 6) of rat *apo*-ACP showed good chemical shift dispersion and HSQC spectra recorded over several weeks showed no observable changes. The overall chemical shift dispersion for the methyl groups of buried aliphatic side-chains was poor. In contrast to other Type II PKS ACPs there are no aromatic residues in rat FAS ACP. As a result a high resolution 3D structure determination was not possible from ^{15}N labeled protein alone and this is currently the subject of further study using ^{13}C–^{15}N labeled protein. Nevertheless almost complete ^{1}H and ^{15}N assignments were obtained for the rat FAS ACP. We observed no unusual chemical shifts with the exception of the δC protons of R67 that are split by 0.3 ppm and the εNH is shifted to 8.66 ppm. All the other arginine εNHs had shifts in the range 7.0–7.5 ppm. There is therefore the suggestion that this side chain proton may be involved in hydrogen bonding to helix 1 in a similar fashion to that observed in the related Type II PKS ACPs studied by NMR in our laboratory.

The NMR short range distance constraints obtained from the ^{15}N labeled rat ACP alone are summarized in Fig. 7. The spectra yielded 41 unambiguous long-range NOEs, along with 165 short-range, 241 sequential and 237 intraresidue NOEs that were sufficient to provide a low resolution assessment of the three dimensional fold. Backbone ϕ angles were determined from $^{3}J_{HNH\alpha}$ coupling constants in a 3D HNHα experiment and 21 dihedral angle restraints were incorporated into structure calculations. The CαH–NH(i,i+3), CαH–NH(i,i+4) NOEs and $^{3}J_{HNH\alpha}$ <6Hz indicate four α-helical regions for rat *apo*-ACP from D8 to I16 (1), G41 to Q51 (2), I58 to Q63 (3) and L66 to S74 (4). At both the *N*- and *C*-termini of the protein, there are large regions (G1 to Q6 and L75 to N89) where no short or long-range NOES were observed. Both regions were characterized by intense CαH–NH(i,i+1) contacts and weak or missing NH–NH(i,i+1) contacts. Indeed after L82 only one contact, apart from the very intense CαH–NH(i,i+1) contacts, was observed.

From an initial set of 30 structures, 24 structures converged with the same global fold after molecular modeling–simulated annealing. This final set was used to generate a single minimized average structure (Fig. 8a). The low resolution of the rat ACP structure is reflected in the fact that the backbone RMSD over residues 8–73 for these 30 structures superimposed on the average structure is 2.1 Å. The backbone RMSDs over the first 8 residues are much higher (7–11 Å) reflecting the complete absence of interresidue non-sequential NOEs involving these residues. With superposition over residues 8–16 and 38–73 (*i.e.* over the four α-helices and the loop between helices 2 and 3), the backbone RMSD drops to 1.8 Å due to the improvement resulting from excluding the poorly-defined loop region between helices 1 and 2. The structure adopted by the polypeptide between helices 1 and 2 (residues 17 to 40) does not conform to an overall motif. Few short-range and no long-range NOEs were observed involving residues 17 to 28 whereas residues 29 to 39 showed many more short-range NOEs and several long-range NOEs involving residues 29 and 30. Thus, while the start of the loop may be flexible and solvent-exposed, after residue 29, the loop is more structured and is packed against the C-terminal of helix 3 and the loop connecting helices 3 and 4.

The core of the protein forms a four helix bundle (Fig. 8a) that is stabilized by the formation of numerous hydrophobic interactions and is typical of other ACP folds. Helix 1 residues L9 and V10 interact with helix 4 and the C-terminus of helix 2. L31 in the more structured part of the loop forms interactions with L64 and T65 in the turn separating helix 3 and 4. However, unlike the Type II *act* ACP[18] and the *Mycobacterium tuberculosis* ACP,[44] there are only two hydrophobic residues present on helix 4, L66 and M72, available to contribute to formation of the hydrophobic core. Residues L74, L75, L77, I78, L82 are present in *act* ACP; and V73,V74 and Y76 in *Mycobacterium tuberculosis* ACP. In rat FAS ACP the L66 packs against the structured part of the loop and the amide of M72 interacts with the methyl groups of L9. We were not, however, able to discern any further interactions along helix 4. The long sequence after M72 (-SSKAGSDTELAAPKSKN-89) contains mainly short side chain or charged amino acids and it is therefore not unexpected that we observe little structuring in this region or interaction with the core of the protein.

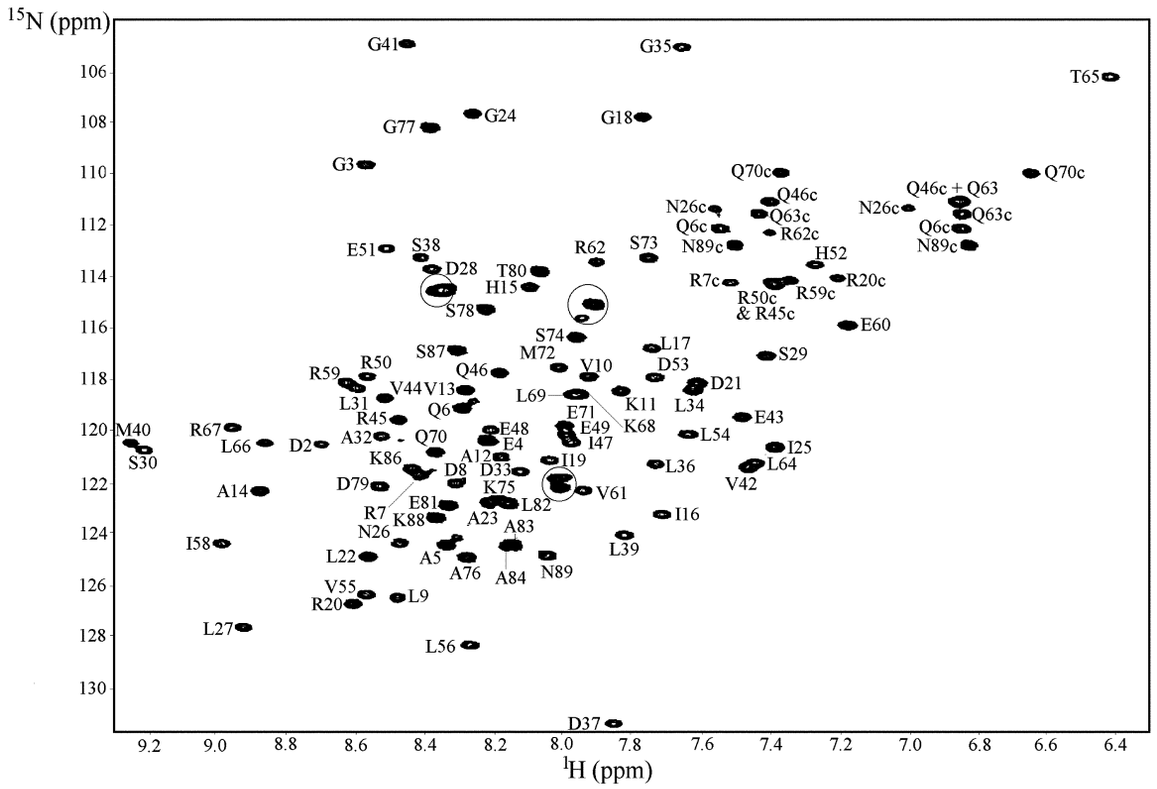

Fig. 6 ^{1}H–^{15}N HSQC spectrum of the *apo*-ACP domain of rat FAS. Assignments marked with a 'c' correspond to side-chain ^{1}H–^{15}N assignments of arginine and glutamine residues. The three circled peaks are impurities that have not been observed in subsequent ^{1}H–^{15}N spectra.

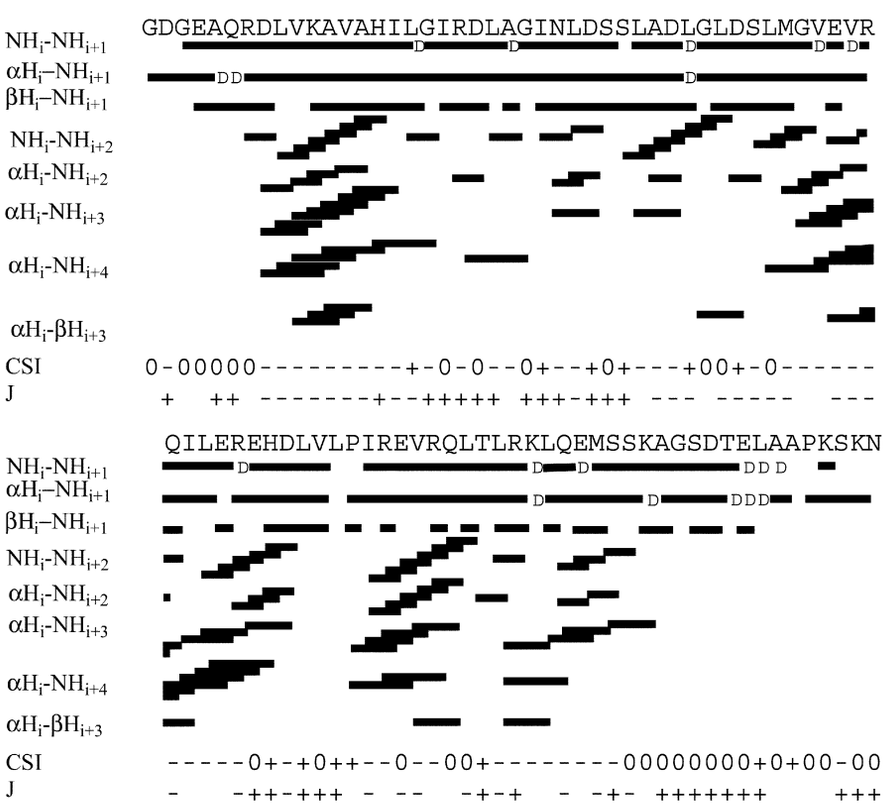

Fig. 7 Summary of the sequential and short range NOEs observed for the Type I rat FAS ACP. $^{3}J_{HN-H\alpha}$ coupling constants (<6Hz) and chemical shift indices (CSIs). For the NOE connectivities a symbol D indicates that an NOE could not be observed in either 2D or 3D data due to overlap of resonances. CSIs of −1, 0, +1 indicate where chemical shifts correlate with α-helix, random coil and β-sheet respectively. Measured $^{3}J_{HN-H\alpha}$ coupling constants <6Hz are indicated by a '−' symbol and >6Hz by a '+' symbol. Spaces indicate that the coupling constant could not be measured due to peak overlap.

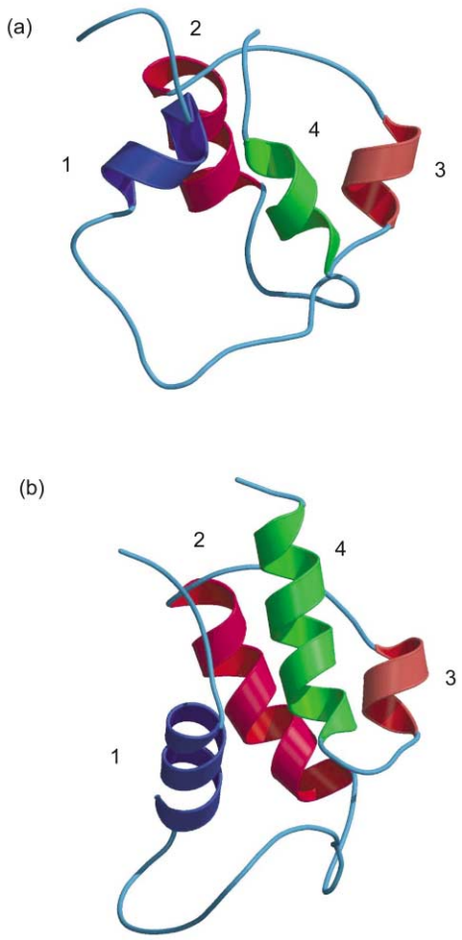

Fig. 8 Ribbon representation and comparison of the global fold of (a) rat FAS ACP and (b) *act* ACP.

3.5 Minimal PKS assay

As previously shown, when the minimal PKS contained C17S *act holo*-ACP, the functional synthase produced a mixture of SEK4 and SEK4b.[28] Substituting the *act* PKS ACP for *holo*-rat FAS ACP abrogated polyketide production. To determine whether this was a problem of malonyl transfer the assay was run in the presence and absence of *S. coelicolor* MCAT. We have already shown that this enzyme is capable of malonylating the heterologous *holo*-rat FAS ACP (*vide supra*). Addition of MCAT, however, did not restore functional activity to the minimal PKS and no polyketides could be detected.

4. Discussion

The rat FAS ACP expressed well in *E. coli* (5 mg L^{-1}) as has been seen previously for other heterologous ACPs (Fig. 1).[35,45] CD analysis shows that the Type I rat FAS ACP has significant α-helical content although we estimate that this may be slightly lower than the Type II *E. coli* FAS or *S. coelicolor act* PKS ACP (Fig. 2). While the shape of its CD spectrum is strongly influenced by the presence of α-helices, the effects of other types of secondary structure are more pronounced than for the two Type II ACPs. The CD analysis showed that the secondary structure of the rat ACP domain is stable at the acidic pH required for extended NMR studies. Comparison of CD spectra over a range of pH values showed that this excised domain appears more stable to acidic pH than the discrete *S. coelicolor act* PKS ACP (Fig. 3). Although charged groups make only a minor contribution to protein stability (compared to hydrophobic interactions, H-bonding and configurational entropy) they are of the order of the total unfolding free energy of the protein.[46] Changes in pH therefore provide a straightforward way of perturbing the unfolding free energy of a protein. Rat FAS ACP has a calculated pI of 5.21[29] compared to 4.0 for *act* ACP.[43] pH Induced unfolding may therefore be expected to occur at a higher pH based on a simple charge accumulation and repulsion model. The observation that rat FAS ACP is in fact more pH stable indicates that a significant component of the free energy difference between the native and denatured states could arise from a small number of amino acids whose pK_as are shifted anomalously in the native protein and form important interactions with charged or polar groups.[47] Similar denaturant concentrations, however, are required to produce the same extent of denaturation for all three ACPs (Fig. 4).[42,43]

The NMR studies described here show that the secondary structure of the rat *apo*-ACP domain comprises four α-helical regions (8–16 [1], 41–51 [2], 58–63 [3] and 66–74 [4]). The initial pattern of long-range NOEs observed for the ACP domain of rat Type I FAS shows strong similarities to the Type II FAS ACPs of *E. coli*,[48] spinach,[15] *B. subtilis*,[16] *M. tuberculosis*[44] and the *S. coelicolor act* PKS ACP[18] suggesting that it forms a small four-helix bundle, the archetypal fold for these proteins. Surprisingly we could only identify 41 long range NOEs using uniformly ^{15}N labeled protein. Compared to other NMR studies of Type II ACPs this figure is low, even when compared to the number of NOEs derived from an unlabelled sample of the Type II *act* ACP from *S. coelicolor* (93 long range NOEs). The number of assigned long-range NOEs for structure calculations was therefore very limited and is principally due to the absence of aromatic residues and subsequent poor chemical shift dispersion of buried aliphatic methyl groups that define the protein core. In the *act* PKS ACP 57% of long-range NOEs involved aromatic residues.[18] We are currently pursuing a high resolution structure determination of the core of this protein using a ^{13}C,^{15}N labeled sample.

Fig. 8 compares the overall low resolution global fold of rat FAS ACP with the *S. coelicolor act* PKS ACP. Although the form of the fold is similar, helices 1 and 4 are shorter than the corresponding regions in the PKS ACP. Consequently, whilst the structured region of the PKS ACP extends for 78 amino acids, the length of the structured ACP domain in rat FAS ACP is only 67 amino acid residues. Nevertheless, the observation of clear secondary structure and tertiary contacts shows, for the first time, that a Type I domain shows strong structural similarities to its Type II counterpart. The lack of structure in the *C*-terminus of the protein (74–89) suggests that this region is part of the peptide linker to the thiolesterase domain of the FAS. There is presently no structural information on these regions in the large multifunctional fatty acid synthases. Recent studies have addressed domain movements in human fatty acid synthase using a computational method that aims to identify flexibility in supermolecular complexes.[49] The model predicts that domains II and III[50] act as a single rigid body, *i.e.* the ER-KR-ACP and TE. This does suggest the ACP and TE interact with each other on the same subunit but provides no insight as yet to the structure of the linker.

Walsh and coworkers suggested that the catalytic efficiency of the *in vitro* phosphopantetheinyl transfer reaction increased with the increasing negative charge on the ACP substrate for the *Streptomyces* ACPs of the *gra*, *fren, otc* and *tcm* PKS.[31] The ACP domain of rat FAS (amino acids 2114–2202) has a negative charge of only 3 at pH 7 whereas the PKS ACPs above have negative charges of at least 11 and *E. coli* FAS ACP, the natural substrate has a negative charge of 15. Therefore, it might be expected that the ACP domain of rat FAS would be a very poor substrate for *E. coli* ACPS. However, co-expression of *E. coli* ACPS and the rat ACP domain gave high yields (approximately 10 mg L^{-1}) of the *holo*-ACP domain in contradiction to previous results.[29] While *E. coli* Type II FAS ACP may be a much better substrate for *E. coli* ACPS than the Type I rat FAS ACP domain, the heterologous ACPS is capable of modifying the ACP domain from the Type I rat FAS. The ACPS

from *S. coelicolor* was also shown to be capable of catalyzing near complete phosphopantetheinyl transfer to the Type I rat FAS ACP domain *in vitro* when present in only a catalytic quantity (0.02 molar equivalents). The *S. coelicolor* ACPS has been previously shown to have a broad substrate specificity which includes both Type I and Type II ACPs. ACPS is also known to be able to transfer acyl phosphopantetheine to the conserved serine of the *apo*-ACP,[30,51] and we found that acetyl *holo* rat FAS ACP could be easily formed using this method. This method of specifically acylating the rat FAS ACP will prove invaluable in the preparation of acyl-ACP substrates which can be used to probe the specificity of other FAS enzymes, as well as determining the structural changes induced in the protein.

During fatty acid and polyketide biosynthesis malonyl groups are normally transferred to the ACP by a malonyl CoA:ACP Transacylase (MCAT) enzyme. The Type I FAS proteins typical of higher organisms possess integral MCAT domains,[52] while the Type II FAS proteins of bacteria and plants use discrete MCAT proteins.[53] MCAT from *E. coli* has been isolated and a three dimensional structure determined.[54] The Type II MCAT isolated from *E. coli* is known to be specific for the transfer of malonate from malonyl CoA, and is capable of transferring this acyl group to heterologous carrier proteins including the nodulation protein from Rhizobium[25] and rat FAS ACP.[29] The *S. coelicolor* MCAT has also recently been characterized, is known to have the same specificity for malonyl CoA, and can acylate a heterologous carrier protein, the FAS ACP from *E. coli*.[36] In this paper we have shown that *S. coelicolor* MCAT will transfer malonate from both CoA as well as the malonyl *N*-acetylcysteamine derivative to the rat FAS ACP. Rates of transfer for malonyl CoA to rat FAS ACP as similar to that seen with the natural *S.coelicolor* FAS ACP substrate, (Fig. 5). Malonyl–SNAC, however, is a much poorer substrate for the MCAT catalysed transfer with a 20-fold increase in substrate concentration needed to obtain equivalent rates of ACP malonylation suggesting that the CoA portion makes a significant contribution to the initial binding of the malonyl CoA.

Clearly the Type I rat FAS ACP possesses a global fold similar to that seen for Type II ACP structures. This protein can also be converted to the active *holo* form and acylated by heterologous Type II enzymes, ACPS and MCAT respectively. A recently published *Bacillus subtilis* ACP/ACPS X-ray structure[20] and modelling studies by Rock and co-workers[21] has given an indication of the protein-protein interactions which are important in these complexes. The X-ray structure of the ACP/ACPS complex clearly shows that negative charges on helix 2 of the ACP interact with positive groups on the ACPS. Fig. 9 shows a sequence pileup of a section of helix 2 of

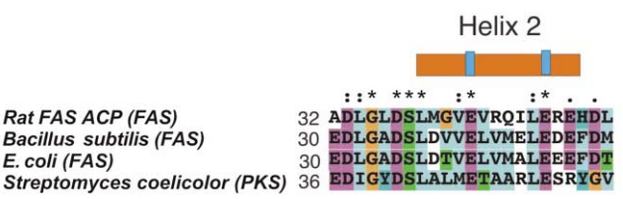

Fig. 9 Sequence alignment of ACPs. The alignment was produced by ClustalX and conserved residues are highlighted with an asterisk. Helix 2 is shown above the sequence.

representative examples of Type I, Type II FAS and PKS ACPs. Acidic residues on this helix may be involved in protein–protein interactions and basic patches have been identified adjacent to the active site enzymes of the *E. coli* FAS enzymes.[21] Rat FAS ACP contains two glutamate residues on helix 2 (E44 and E50) in the same positions as the other ACPs indicated. It is therefore extremely interesting to note the possibility that a Type I ACP may interact with ACPS as well as other FAS proteins in a similar fashion to a Type II ACP. Given the similarities in ACP three-dimensional structure it would seem reasonable in some circumstances that one carrier protein may be substituted with another. This has been suggested for the PKS complex where attempts have been made to replace the normal *act* ACP (both *in vivo*[24] and *in vitro*[51]) with ACP homologues from other PKS complexes, as well as the *Saccharopolyspora erythraea* FAS ACP to generate potentially functional systems. More recent studies have indicated that heterologous ACP substitutions are not always possible, for example, polyketide ACPs are inactive in *E. coli* acyl-ACP synthase assays,[26] while both the rhizobium nodulation protein[25] and the tetracenomycin PKS ACP[27] were not substrates for the enzyme KAS III, which initiates fatty acid biosynthesis in Type II systems. We have previously shown that replacement of a Type II PKS ACP with a Type II FAS ACP in a PKS minimal system completely abolishes polyketide production.[28] In this paper the Type I rat FAS ACP was also incapable of replacing the Type II *act* ACP in the *S. coelicolor in vitro* minimal system either in the presence or absence of MCAT. This contradicts a previous *in vivo* report.[29] This shows that although the gross three-dimensional structures of ACPs are similar, subtle differences exist which may perturb either protein-substrate, or protein-protein interactions. We are currently closely examining the structures of a number of Type I and Type II ACPs from both FAS and PKS in order to more fully understand these differences.

Acknowledgements

This work was supported by the Biotechnology and Biological Sciences Research Council (BBSRC – grant number 7/B11480). Studentships from the BBSRC (M.A.C.R and C.A) and the University of Bristol and ORSAS (A.E.S) are gratefully acknowledged. We thank PENCE (Canada) for spectrometer time and the Wellcome Trust (Equipment Grant 055640) for the provision of a 600 MHz spectrometer at Southampton.

References

1 M. Rawlings and J. E. Cronan, *J. Biol. Chem.*, 1992, **267**, 5751–5754.
2 S. R. Baerson, M. G. Vanderheiden and G. K. Lamppa, *Plant Mol.Biol.*, 1994, **26**, 1947–1959.
3 G. Ragone, R. Caizzi, R. Moschetti, P. Barsanti, V. De Pinto and C. Caggese, *Mol. Gen. Genet.*, 1999, **261**, 690–697.
4 S. Smith, *FASEB J.*, 1994, **8**, 1248–1259.
5 D. H. Keating, M. R. Carey and J. E. Cronan, *J. Biol. Chem.*, 1995, **270**, 22229–22235.
6 K. Magnuson, S. Jackowski, C. O. Rock and J. E. Cronan, *Microbiol. Rev.*, 1993, **57**, 522–542.
7 S. J. Wakil, *Biochemistry*, 1989, **28**, 4523–4530.
8 R. H. Lambalot, A. M. Gehring, R. S. Flugel, P. Zuber, M. LaCelle, M. A. Marahiel, R. Reid, C. Khosla and C. T. Walsh, *Chem. Biol.*, 1996, **3**, 923–936.
9 D. A. Hopwood, *Chem. Rev.*, 1997, **97**, 2465–2497.
10 T. Weber and M. A. Marahiel, *Structure*, 2001, **9**, R3–R9.
11 T. H. Grossman, M. Tuckman, S. Ellestad and M. S. Osburne, *J. Bacteriol.*, 1993, **175**, 6203–6211.
12 H. P. Spaink, D. M. Sheeley, A. A. N. Vanbrussel, J. Glushka, W. S. York, T. Tak, O. Geiger, E. P. Kennedy, V. N. Reinhold and B. J. J. Lugtenberg, *Nature*, 1991, **354**, 125–130.
13 D. V. Debabov, M. Y. Kiriukhin and F. C. Neuhaus, *J. Bacteriol.*, 2000, **182**, 2855–2864.
14 M. Andrec, R. B. Hill and J. H. Prestegard, *Protein Sci.*, 1995, **4**, 983–993.
15 M. C. Oswood, Y. Kim, J. B. Ohlrogge and J. H. Prestegard, *Proteins*, 1997, **27**, 131–143.
16 G. Y. Xu, A. Tam, L. Lin, J. Hixon, C. C. Fritz and R. Powers, *Structure*, 2001, **9**, 277–287.
17 R. Ghose, O. Geiger and J. H. Prestegard, *FEBS Lett.*, 1996, **388**, 66–72.
18 M. P. Crump, J. Crosby, C. E. Dempsey, J. A. Parkinson, M. Murray, D. A. Hopwood and T. J. Simpson, *Biochemistry*, 1997, **36**, 6000–6008.
19 T. Weber, R. Baumgartner, C. Renner, M. A. Marahiel and T. A. Holak, *Struct. Fold. Des.*, 2000, **8**, 407–418.

20 K. D. Parris, L. Lin, A. Tam, R. Mathew, J. Hixon, M. Stahl, C. C. Fritz, J. Seehra and W. S. Somers, *Struct. Fold. Des.*, 2000, **8**, 883–895.
21 Y. M. Zhang, M. S. Rao, R. J. Heath, A. C. Price, A. J. Olson, C. O. Rock and S. W. White, *J. Biol. Chem.*, 2001, **276**, 8231–8238.
22 A. Roujeinikova, C. Baldock, W. J. Simon, J. Gilroy, P. J. Baker, A. R. Stuitje, D. W. Rice, A. R. Slabas and J. B. Rafferty, *Structure*, 2002, **10**, 825–835.
23 R. J. Cox, J. Crosby, O. Daltrop, F. Glod, M. E. Jarzabek, T. P. Nicholson, M. Reed, T. J. Simpson, L. H. Smith, F. Soulas, A. E. Szafranska and J. Westcott, *J. Chem. Soc., Perkin Trans. 1*, 2002, 1644–1649.
24 C. Khosla, S. Ebertkhosla and D. A. Hopwood, *Mol. Microbiol.*, 1992, **6**, 3237–3249.
25 T. Ritsema, A. M. Gehring, A. R. Stuitje, K. van der Drift, I. Dandal, R. H. Lambalot, C. T. Walsh, J. E. Thomas-Oates, B. J. J. Lugtenberg and H. P. Spaink, *Mol. Gen. Genet.*, 1998, **257**, 641–648.
26 J. Crosby, K. J. Byrom, T. S. Hitchman, R. J. Cox, M. P. Crump, I. S. C. Findlow, M. J. Bibb and T. J. Simpson, *FEBS Lett.*, 1998, **433**, 132–138.
27 G. Florova, G. Kazanina and K. A. Reynolds, *Biochemistry*, 2002, **41**, 10462–10471.
28 A. L. Matharu, R. J. Cox, J. Crosby, K. J. Byrom and T. J. Simpson, *Chem. Biol.*, 1998, **5**, 699–711.
29 S. Tropf, W. P. Revill, M. J. Bibb, D. A. Hopwood and M. Schweizer, *Chem. Biol.*, 1998, **5**, 135–146.
30 R. J. Cox, T. S. Hitchman, K. J. Byrom, I. S. C. Findlow, J. A. Tanner, J. Crosby and T. J. Simpson, *FEBS Lett.*, 1997, **405**, 267–272.
31 A. M. Gehring, R. H. Lambalot, K. W. Vogel, D. G. Drueckhammer and C. T. Walsh, *Chem. Biol.*, 1997, **4**, 17–24.
32 C. W. Carreras and C. Khosla, *Biochemistry*, 1998, **37**, 2084–2088.
33 S. A. Morris, W. P. Revill, J. Staunton and P. F. Leadlay, *Biochem. J.*, 1993, **294**, 521–527.
34 R. L. Winston and M. C. Fitzgerald, *Anal. Biochem.*, 1998, **262**, 83–85.
35 J. Crosby, D. H. Sherman, M. J. Bibb, W. P. Revill, D. A. Hopwood and T. J. Simpson, *Biochim. Biophys. Acta-Protein Struct. Molec. Enzym.*, 1995, **1251**, 32–42.
36 A. E. Szafranska, T. S. Hitchman, R. J. Cox, J. Crosby and T. J. Simpson, *Biochemistry*, 2002, **41**, 1421–1427.
37 C. Arthur, R. J. Cox, J. Crosby, M. M. Rahman, T. J. Simpson, F. Soulas, R. Spogli, A. E. Szafranska, J. Westcott and C. J. Winfield, *ChemBioChem*, 2002, **3**, 253–257.
38 L. M. Rice and A. T. Brunger, *Proteins*, 1994, **19**, 277–290.
39 M. Nilges, A. M. Gronenborn, A. T. Brunger and G. M. Clore, *Protein Eng.*, 1988, **2**, 27–38.
40 R. A. Laskowski, M. W. Macarthur, D. S. Moss and J. M. Thornton, *J. Appl. Crystallogr.*, 1993, **26**, 283–291.
41 W. C. Johnson, *Proteins*, 1999, **35**, 307–312.
42 T. Takagi and C. Tanford, *Proteins*, 1968, **19**, 277–290.
43 M. P. Crump, PhD Thesis, 1995, School of Chemistry, University of Bristol.
44 H. C. Wong, G. H. Liu, Y. M. Zhang, C. O. Rock and J. Zheng, *J. Biol. Chem.*, 2002, **277**, 15874–15880.
45 W. P. Revill and P. F. Leadlay, *J. Bacteriol.*, 1991, **173**, 4379–4385.
46 P. L. Privalov and S. J. Gill, *Adv. Protein Chem.*, 1988, **39**, 191–234.
47 C. N. Pace, D. V. Laurents and J. A. Thomson, *Biochemistry*, 1990, **29**, 2564–2572.
48 T. A. Holak, M. Nilges and H. Oschkinat, *FEBS Lett.*, 1989, **242**, 218–224.
49 D. Ming, Y. F. Kong, M. A. Lambert, Z. Huang and J. P. Ma, *Proc. Natl. Acad. Sci. U. S. A.*, 2002, **99**, 8620–8625.
50 J. Brink, S. J. Ludtke, C. Y. Yang, Z. W. Go, S. J. Wakil and W. Chiu, *Proc. Natl. Acad. Sci. U. S. A.*, 2002, **99**, 138–143.
51 C. W. Carreras, A. M. Gehring, C. T. Walsh and C. Khosla, *Biochemistry*, 1997, **36**, 11757–11761.
52 A. K. Joshi, A. Witkowski and S. Smith, *Biochemistry*, 1998, **37**, 2515–2523.
53 F. E. Ruch and P. R. Vagelos, *J. Biol. Chem.*, 1973, **248**, 8095–8106.
54 L. Serre, E. C. Verbree, Z. Dauter, A. R. Stuitje and Z. S. Derewenda, *J. Biol. Chem.*, 1995, **270**, 12961–12964.
55 E. A. Bienkiewicz and R. W. Woody, *Biospectroscopy*, 1997, **3**, 171–181.